

Interactions in hypoxic and hypercapnic breathing are genetically linked to mouse chromosomes 1 and 5

Clarke G. Tankersley¹ and Karl W. Broman²

Departments of ¹Environmental Health Sciences and ²Biostatistics, The Johns Hopkins University, Bloomberg School of Public Health, Baltimore, Maryland 21205

Submitted 10 October 2003; accepted in final form 16 February 2004

Tankersley, Clarke G., and Karl W. Broman. Interactions in hypoxic and hypercapnic breathing are genetically linked to mouse chromosomes 1 and 5. *J Appl Physiol* 97: 77–84, 2004. First published February 20, 2004; 10.1152/jappphysiol.01102.2003.—The genetic basis for differences in the regulation of breathing is certainly multigenic. The present paper builds on a well-established genetic model of differences in breathing using inbred mouse strains. We tested the interactive effects of hypoxia and hypercapnia in two strains of mice known for variation in hypercapnic ventilatory sensitivity (HCVS); i.e., high gain in C57BL/6J (B6) and low gain in C3H/HeJ (C3) mice. Strain differences in the magnitude and pattern of breathing were measured during normoxia [inspired O₂ fraction (F_IO₂) = 0.21] and hypoxia (F_IO₂ = 0.10) with mild or severe hypercapnia (inspired CO₂ fraction = 0.03 or 0.08) using whole body plethysmography. At each level of F_IO₂, the change in minute ventilation (\dot{V}_E) from 3 to 8% CO₂ was computed, and the strain differences between B6 and C3 mice in HCVS were maintained. Inheritance patterns showed potentiation effects of hypoxia on HCVS (i.e., CO₂ potentiation) unique to the B6C3F1/J offspring of B6 and C3 progenitors; i.e., the change in \dot{V}_E from 3 to 8% CO₂ was significantly greater ($P < 0.01$) with hypoxia relative to normoxia in F1 mice. Linkage analysis using intercross progeny (F2; $n = 52$) of B6 and C3 progenitors revealed two significant quantitative trait loci associated with variable HCVS phenotypes. After normalization for body weight, variation in \dot{V}_E responses during 8% CO₂ in hypoxia was linked to mouse chromosome 1 (logarithm of the odds ratio = 4.4) in an interval between 68 and 89 cM (i.e., between *D1Mit14* and *D1Mit291*). The second quantitative trait loci linked differences in CO₂ potentiation to mouse chromosome 5 (logarithm of the odds ratio = 3.7) in a region between 7 and 29 cM (i.e., centered at *D5Mit66*). In conclusion, these results support the hypothesis that a minimum of two significant genes modulate the interactive effects of hypoxia and hypercapnia in this genetic model.

C3H/HeJ; C57BL/6J; carbon dioxide potentiation; control of breathing; linkage analysis

THE INTERACTIVE MECHANISMS that regulate breathing during coexposure to hypercapnic and hypoxic inspirates are complex and may involve multiple chemoreceptive pathways. It is generally accepted, however, that human subjects (20) and other larger mammalian species (8, 10) show an increased slope of the hypercapnic ventilatory sensitivity (HCVS) curve when the O₂ tension is simultaneously lowered. In one study, Kobayashi et al. (17) suggested that genetic factors were important in determining variation in HCVS responses when measured with admixtures of hypoxia. In a study of twins, these investigators measured the neural drive during CO₂ stimulation (i.e., the ratio between inspiratory mouth pressure

after 0.1 s of occlusion and the end-tidal CO₂) and the HCVS [i.e., the slope of minute ventilation (\dot{V}_E) to end-tidal CO₂] while O₂ levels were lowered. Concordance between monozygotic twins was greatest relative to dizygotic twins for HCVS phenotypes in hypoxic admixtures. Similar concordance in HCVS phenotypes was not observed in the presence of hyperoxic admixtures. The concordance pattern indicates that robust genetic factors modulate breathing during hypercapnic and hypoxic interactions.

Another approach to studying such genetic factors (modulating breathing during hypercapnic and hypoxic interactions) is to determine the origin of variation among different inbred strains of mice. Our laboratory has focused on C3H/HeJ (C3) and C57BL/6J (B6) inbred strains because the breathing characteristics at baseline (i.e., room air) and during acute hypoxic and hypercapnic stimulation are most different relative to other inbred strains (38). Complementary studies, including cross-breeding strategies and quantitative genetic approaches, demonstrated phenotypic variation among first-generation offspring derived from C3 and B6 parental strains (41–43). Inheritance patterns, using backcross and intercross (F2) offspring of C3 and B6 progenitors, suggested that specific breathing traits at baseline and during acute hypoxia were modulated by a modest number of major genes (39, 40). Subsequent linkage analysis identified two quantitative trait loci (QTL) that linked variation in specific breathing phenotypes to genomic regions on mouse chromosomes 3 and 9 (33, 34, 36). Hence, a QTL on chromosome 3 regulates differences in the inspiratory timing (T_I) at baseline (i.e., the *Itbq1* locus). Another QTL on chromosome 9 regulates variation in acute hypoxic ventilatory responses [i.e., tidal volume (V_T), \dot{V}_E , and mean inspiratory flow (V_T/T_I)] during an inspirate challenge of 10% O₂ and 3% CO₂.

The purpose of the present study is to advance our QTL analysis by using the C3 and B6 variation in HCVS and consider the possible genetic determinants that modulate the regulation of breathing during hypercapnic and hypoxic interactions. To achieve these aims, a genome-wide screen was performed with 176 microsatellite markers to analyze DNA samples from 52 F2 offspring. F2 offspring were previously characterized with respect to eupneic and hypoxic breathing characteristics (37, 39). Considering that there are multiple CO₂ and O₂ chemosensory and transducing pathways, the hypothesis of the present study suggests that the genetic bases for variation in hypercapnic breathing characteristics differ from those regulating eupneic and hypoxic breathing. The

Address for reprint requests and other correspondence: C. G. Tankersley, Division of Physiology, Bloomberg School of Public Health, The Johns Hopkins University, 615 N. Wolfe St., Baltimore, MD 21205.

The costs of publication of this article were defrayed in part by the payment of page charges. The article must therefore be hereby marked "advertisement" in accordance with 18 U.S.C. Section 1734 solely to indicate this fact.

results demonstrate candidate genomic regions on mouse chromosomes 1 and 5. These chromosomes contain genes that modulate phenotypic variation in hypercapnic \dot{V}_E and V_T and influence the interaction between CO₂ and O₂ chemosensory and transduction mechanisms in this genetic model.

METHODS

Animals. Reproductively mature male and female C3 and B6 inbred progenitors, and the B6C3F1/J (F1) mice were purchased from Jackson Laboratory (Bar Harbor, ME) to establish breeding colonies at the Johns Hopkins School of Public Health. Two backcross [i.e., B6 female \times F1 male (BXB6); and, C3 female \times F1 male (BXC3)] and intercross progeny [i.e., F1 progenitors (F2)] were generated and weaned at 4–5 wk of age. Male BXB6 ($n = 35$), BXC3 ($n = 20$), and F2 ($n = 69$) offspring were randomly selected from the breeding colonies and housed in cages of four to six animals for an additional 6–12 wk. Water and mouse chow (Agway Pro-Lab RMH 1000) were provided ad libitum. All animal protocols were reviewed and approved by the Animal Care and Use Committee of the Johns Hopkins School of Public Health.

HCVS. The magnitude and pattern of ventilation was determined by whole body plethysmography using unrestrained and unanesthetized conditions. Detailed methods and results have been reported elsewhere (37, 38). Briefly, ventilatory function was evaluated during the following sequence of acute (3–5 min) inspiratory challenges [inspired CO₂ fraction (F_{ICO₂})-inspired O₂ fraction (F_{IO₂}) in N₂]: 1) mild hypercapnic hypoxia, 0.03 CO₂-0.10 O₂; 2) mild hypercapnic normoxia, 0.03 CO₂-0.21 O₂; 3) severe hypercapnic hypoxia, 0.08 CO₂-0.10 O₂; and 4) severe hypercapnic normoxia, 0.08 CO₂-0.21 O₂. Each challenge was followed by exposure to room air to ensure that responses to ventilatory challenges were generated from similar pre-exposure levels. In general, baseline breathing characteristics were reestablished after 15–20 min of room air exposure. The animals were weighed after each protocol.

The analog signal generated from a pressure transducer attached to the plethysmograph was recorded as digital input with a data acquisition system (Keithley Instruments) and a dedicated computer. The data were acquired at an input frequency of 100 Hz, and peak inspiration and expiration were determined from at least 15 consecutive tidal breaths. The analog signal was also captured by a strip-chart recorder (model 7D, Grass Polygraph) in the event that the computer did not secure a particular breathing sample. From each sample, breathing frequency (f), V_T , and T_I were directly measured. The product of f and V_T was calculated to equal \dot{V}_E . Expiratory time was determined from the reciprocal of f (T_{tot}) minus T_I , mean inspiratory flow was calculated as the ratio of V_T to T_I , and the inspiratory fraction was computed as the ratio of T_I to T_{tot} . The slope of the HCVS curve was estimated during both normoxic and hypoxic conditions by determining the difference in \dot{V}_E response between CO₂ levels of 3 and 8%. An indicator of CO₂ potentiation was defined by an increase in the slope of the HCVS curve from normoxia to hypoxia. The V_T/T_I and T_I/T_{tot} components of \dot{V}_E were used to identify the “driver” and “timer” elements (21), respectively, as a general model of respiratory control mechanisms. Each one of the ventilatory characteristics was compared with room air breathing to evaluate relevant percent change.

In the present study, \dot{V}_E and V_T responses during severe hypercapnic hypoxia were notably correlated with body weight in the progenitor strains and second-generation offspring. Therefore, linear regression and correlational analyses were used to focus attention on estimating the influence of body weight on ventilatory responses. Although the results from these analyses were significant within parental strains and certain offspring classes, the body weight influence on between-strain variability or on the relative distributions of responses in segregant offspring was not substantial. Nevertheless, the results from linkage analysis were computed after ventilatory re-

sponses were normalized for individual differences in body weight. Body weight adjustments did not affect the computations for HCVS or for indexes of CO₂ potentiation.

DNA isolation. After the ventilatory measurements, DNA samples were isolated from kidney tissue of 52 randomly selected F2 mice. To isolate high molecular weight DNA (26), sample tissue was gently homogenized using a Dounce homogenizer in an isotonic, high-pH solution that included Nonidet P-40. To release genomic DNA, nuclear membranes were lysed in a SDS-proteinase K solution. After incubation at 42°C for 3 h, DNA was separated from other cellular components by extraction with a phenol-chloroform-isoamyl alcohol solution. DNA was precipitated with ice-cold 95% ethanol and 0.15 M potassium chloride. Sample DNA was spooled on a glass rod, rinsed with 70% ethanol, and stored in Tris-EDTA buffer (pH = 8.0). We determined the purity of the sample DNA using spectrophotometry and calculating the ratio of optical densities at wavelengths of 260 and 280 nm (i.e., a target 260-nm-to-280-nm optical density ratio of 1.8).

PCR amplification. Primers surrounding DNA microsatellite markers ($n = 176$) polymorphic between C3 and B6 mice were purchased from Research Genetics (Huntsville, AL). The primers were used to amplify sample DNA. One primer from each pair was end-labeled with γ -³²P using the following reaction conditions: 5.4 μ l of sterile H₂O; 3.6 μ l of 5 \times kinase buffer [final concentration equal to 0.25 M Tris (pH = 9.0), 0.05 M MgCl₂, 0.05 M dithiothreitol, 0.25 mg/ml bovine serum albumin]; 4.3 μ l of primer (10 μ M); 0.7 μ l of T4 polynucleotide kinase (7 units); and 4 μ l of [γ -³²P]ATP. The solution was incubated at 37°C for 1 h and diluted with 26 μ l of sterile H₂O followed by column purification to remove unincorporated γ -³²P.

In general, PCR was performed with the following reaction conditions (final volume of 12.5 μ l): 1 μ l of sample DNA (80 ng); 1.25 μ l of 10 \times PCR buffer [final concentration of 500 mM KCl, 100 mM Tris (pH = 8.3), and 1.5 mM MgCl₂]; 0.5 μ l of deoxyribonucleotide triphosphates (equal volumes of dATP, dCTP, dGTP, and dTTP at 2.5 mM each); 0.5 μ l of unlabeled primer (10 μ M); 0.5 μ l of labeled primer (1.5 μ M); 0.1 μ l of *Taq* polymerase (0.25 U); and 8.65 μ l of sterile H₂O. The thermocycler (Perkin Elmer 9600) was programmed to sequentially run linked files as follows: 1) 94°C for 10 min; 2) 30 three-step cycles, consisting of denaturation at 94°C for 30 s, annealing at a temperature optimized for each primer set for 30 s, elongation at 72°C for 30 s; 3) final extension phase at 72°C for 7 min; and 4) a soak phase at 4°C.

Acrylamide (6%) denaturing gels were used to separate single strands of amplified DNA according to size. Appropriate PCR controls (i.e., B6, C3, and F1 DNA and no DNA) were used to ensure proper sample loading and to establish the absence of DNA contamination. The genotypes of the F2 offspring were determined by comparing the allelic size of the simple sequence repeat to the known DNA allele size of the parental strains.

Marker selection and linkage analysis. At the time of this study, ~500 PCR-based markers were available throughout the mouse genome that differed between C3 and B6 strains. Markers were selected to establish 10- to 15-centimorgans (cM) intervals between two loci and to provide complete coverage of the mouse genome.

Quantitative trait linkage analysis was performed using the software R/qtl (5), an add-on package for the statistical software R (13). We used standard interval mapping approaches, as well as a modified version in which adjustment was made for body weight via the algorithm for composite interval mapping (36, 47, 48).

More specifically, in the standard interval mapping approach, we consider each genomic position, one at a time, as the location for a single putative QTL. Individuals with QTL genotype g are assumed to have a phenotype that is normally distributed with mean μ_g (depending on the QTL genotype) and standard deviation σ (independent of the QTL genotype). Although the QTL genotypes are generally not known, one may calculate the conditional QTL probabilities, given the available multipoint marker genotype data. Evidence for the presence of a QTL was measured via the LOD score, the log₁₀

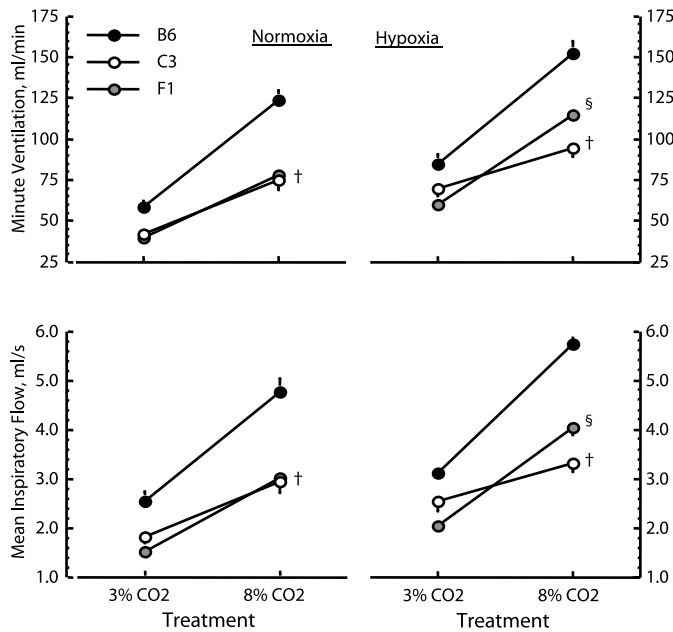


Fig. 1. Average (\pm SE) minute ventilation (\dot{V}_E) and mean inspiratory flow (V_T/T_I) responses are depicted for the C3 and B6 progenitors ($n = 20$ mice/strain) and their F1 offspring ($n = 14$ mice). Average \dot{V}_E and V_T/T_I responses to incremental hypercapnic challenge in normoxia are significantly ($P < 0.01$) greater in the B6 strain compared with both C3 and F1 mice. See text for definitions of mouse strains. Whereas F1 mice show significantly ($P < 0.01$) reduced \dot{V}_E and V_T/T_I responses at low CO₂ levels in hypoxia compared with the progenitors, the \dot{V}_E and V_T/T_I responses are intermediate during high CO₂ levels in hypoxia; i.e., the \dot{V}_E and V_T/T_I responses are significantly ($P < 0.01$) greater than C3 mice yet remain significantly ($P < 0.01$) reduced relative to B6 mice. † $P < 0.01$ vs. B6 strain. § $P < 0.01$ vs. B6 and C3 strains.

likelihood ratio comparing the hypothesis of a single QTL at the specified position to the hypothesis of no QTL anywhere (i.e., that the individuals' phenotypes follow a single normal distribution).

In the modified version of standard interval mapping, in which adjustment was made for body weight, we assumed that an individual with QTL genotype g and body weight w had a phenotype that was normally distributed with mean $\alpha_g + \beta w$ and standard deviation σ . For both versions of the analysis, statistical significance was determined by permutation testing with 1,000 permutation replicates (9).

The summary results reported in Fig. 1 and Table 1 are means and SE. These data were analyzed using a one-way ANOVA to determine strain effects. Post hoc mean comparisons were performed, and statistical significance was established at an α level of 0.01.

RESULTS

As shown in Fig. 1, *left*, the average ventilatory responses to incremental hypercapnic challenge in normoxia are significantly ($P < 0.01$) greater in the B6 strain compared with both the C3 progenitor and the F1 offspring. For the B6 strain, the brisk increase in \dot{V}_E results from a rapid and deep breathing pattern; f is significantly ($P < 0.01$) greater relative to C3 mice and V_T is significantly ($P < 0.01$) greater relative to F1 mice at each level of CO₂ challenge (see Table 1). As a result, the V_T-T_I response in B6 mice is significantly ($P < 0.01$) greater than both C3 and F1 mice at each CO₂ level.

In Fig. 1, *right*, the ventilatory responses to incremental hypercapnic challenge in hypoxia are shown for C3, B6, and F1 mice. In this case, the average \dot{V}_E response in C3 mice is significantly ($P < 0.01$) lower than B6 mice at each level of CO₂. In contrast to normoxia, F1 mice show a significantly ($P < 0.01$) depressed response at low CO₂ levels in hypoxia compared with both progenitors. During high CO₂ levels in hypoxia, however, the \dot{V}_E response in F1 mice is intermediate compared with the progenitors; i.e., the \dot{V}_E response is significantly ($P < 0.01$) greater than in C3 mice yet remains significantly ($P < 0.01$) reduced relative to B6 mice. F1 mice achieve a greater \dot{V}_E response at high CO₂ levels with hypoxia by significantly augmenting V_T and V_T-T_I responses compared with C3 mice (see Table 1).

In Fig. 2, correlational plots illustrate the relationships between \dot{V}_E responses at high CO₂ levels in hypoxia and body weight for C3 and B6 progenitors, and their first- and second-generation offspring. In Fig. 2, *top*, the progenitors show a significant positive correlation ($r = 0.63$; $P < 0.01$), suggesting that \dot{V}_E responses increase as a function of body weight. The same relationship between \dot{V}_E responses and body weight is not evident in F1 mice ($r = 0.01$; $P > 0.05$). Although the results suggest that body weight positively influences the \dot{V}_E responses at high CO₂ levels in hypoxia for C3 and B6 mice,

Table 1. Strain variation in hypercapnic (8% CO₂) ventilatory characteristic among C3, B6, and F1 mice

Strain	Age, days	Weight, g	f, Hz	V_T , μ l	V_T , μ l/g	\dot{V}_E , ml/min	\dot{V}_E , ml \cdot min ⁻¹ \cdot g ⁻¹	T_I , s	T_E , s	V_T/T_I , ml/s	T_I/T_{tot} , %
<i>Normoxia</i>											
C3H/HeJ	$n = 20$	82.2 \pm 4.0	25.2 \pm 0.6	3.18 \pm 0.08†	385.6 \pm 21.8	15.2 \pm 0.7	74.7 \pm 5.6†	0.133 \pm 0.003*	0.185 \pm 0.006†	2.95 \pm 0.21†	41.9 \pm 0.5
		78.4 \pm 3.5	26.4 \pm 0.8	5.45 \pm 0.08	376.5 \pm 16.5	14.2 \pm 0.4	123.4 \pm 6.0	0.080 \pm 0.002	0.104 \pm 0.002	4.79 \pm 0.26	43.2 \pm 0.5
B6C3F1	$n = 14$	61.4 \pm 1.4*	25.2 \pm 0.4	4.83 \pm 0.11*	267.9 \pm 8.1*	10.6 \pm 0.3*	77.8 \pm 3.2†	0.089 \pm 0.001	0.120 \pm 0.004*	3.03 \pm 0.10†	47.5 \pm 0.4
		<i>Hypoxia</i>									
C3H/HeJ				4.12 \pm 0.08*	382.3 \pm 19.8†	15.1 \pm 0.6	94.5 \pm 5.2†	0.116 \pm 0.002*	0.128 \pm 0.003*	3.31 \pm 0.18†	47.6 \pm 0.4†
				5.86 \pm 0.06	434.2 \pm 18.9	16.4 \pm 0.5	152.5 \pm 6.8	0.076 \pm 0.001	0.095 \pm 0.002	5.74 \pm 0.29	44.5 \pm 0.5
B6C3F1				5.84 \pm 0.08	327.1 \pm 8.3*	13.0 \pm 0.4*	114.7 \pm 3.6*	0.082 \pm 0.001	0.090 \pm 0.002	4.03 \pm 0.13*	47.5 \pm 0.4†

Values are means \pm SE. f, Breathing frequency; V_T , tidal volume; \dot{V}_E , minute ventilation; T_I , inspiratory timing; T_E , expiratory time; V_T/T_I , mean inspiratory flow; T_{tot} , reciprocal of f; T_I/T_{tot} , inspiratory fraction. † $P < 0.01$ vs. the C57BL/6J (B6) strain. * $P < 0.01$ vs. other 2 strains.

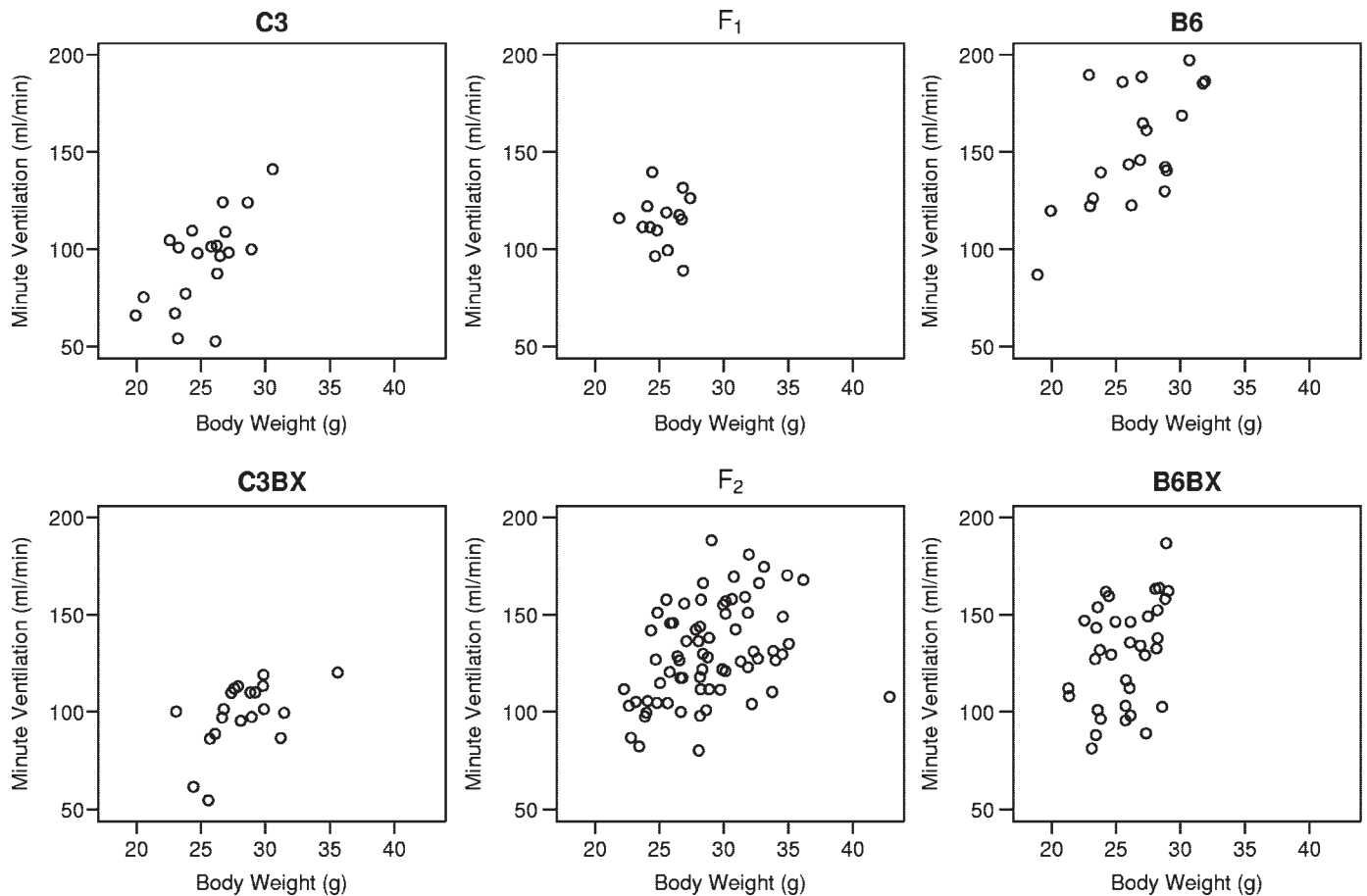


Fig. 2. Correlational plots depict the relationships between \dot{V}_E during hypercapnic hypoxia and body weight for the C3 and B6 progenitors and their first- and second-generation offspring. The relationships are robust in the progenitors ($r = 0.63$; $P < 0.01$) and C3BX ($r = 0.53$; $P < 0.05$) but not for F1, B6BX, or F2 progeny.

the between-strain variation in ventilatory responses evident in Fig. 1 is preserved among the progenitors and F1 mice. In Fig. 2, *bottom*, similar correlational plots are shown for three groups of second-generation offspring of C3 and B6 progenitors. The relationship between \dot{V}_E responses at high CO₂ levels in hypoxia and body weight is robust ($r = 0.53$; $P < 0.05$) in C3BX mice; however, \dot{V}_E responses are not as greatly influenced by body weight in B6BX or F2 mice ($r = 0.38$; $P > 0.05$). Collectively, these data suggest that the segregation of \dot{V}_E phenotypes within B6BX and F2 offspring is attributable to variation in body weight to a lesser extent than in the progenitors and C3BX mice.

In Fig. 3, segregation plots illustrate differences in \dot{V}_E (i.e., normalized to body weight) from low to high CO₂ levels in normoxia (Fig. 3A) and hypoxia (Fig. 3B) for the progenitors and first- and second-generation offspring. In normoxia, there is modest overlap in the distributions of \dot{V}_E differences for the progenitors. The individual \dot{V}_E differences in F1 mice fall within the range of C3 mice. The distribution of responses for C3BX mice also falls within the C3 range; however, B6BX and F2 response distributions are much broader, encompassing both parental ranges.

In hypoxia, individual \dot{V}_E differences among the progenitors resemble the corresponding normoxic results, but B6 responses are more broadly distributed, and F1 responses are shifted

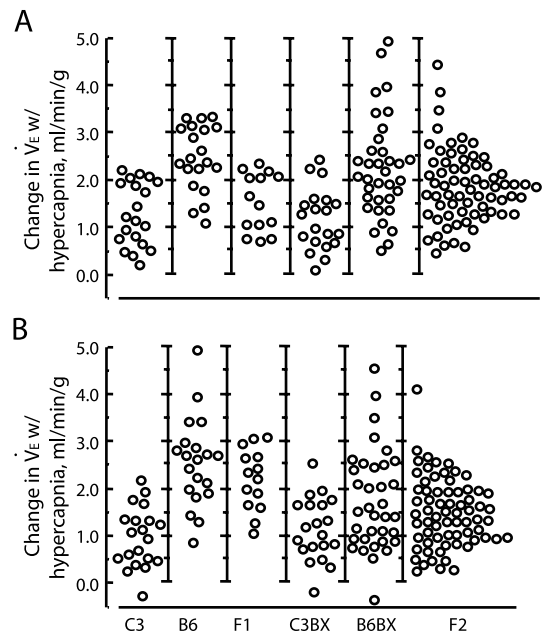


Fig. 3. Segregation plots of \dot{V}_E response differences from low to high CO₂ levels in normoxia (A) and hypoxia (B) are illustrated for the C3 and B6 progenitors and their first- and second-generation offspring. In normoxia, the individual \dot{V}_E differences in F1 mice fall within the range of C3 mice but are shifted above the range of C3 mice to an intermediate phenotype in hypoxia.

above the range of C3 mice to an intermediate phenotype. The C3BX responses are again maintained within the C3 range, and B6BX and F2 response appear to parallel corresponding normoxic differences.

As shown in Fig. 4, individual responses indicative of CO₂ potentiation are plotted for the progenitors and first- and second-generation offspring. The hatched-line demarcates the number of individual responses conferring CO₂ potentiation phenotypes. Although C3 and B6 progenitors show equal numbers of individuals with CO₂ potentiation, all F1 responses consistently manifested CO₂ potentiation phenotypes. These data strongly suggest that there are heritable genetic determinants derived from C3 and B6 progenitors, which confer greater CO₂ ventilatory sensitivity during hypoxia relative to normoxia. Responses consistent with CO₂ potentiation phenotypes are also observed in second-generation offspring. For example, as many as 30% of the F2 responses show CO₂ potentiation phenotypes.

Figure 5 shows LOD plots linking variation in \dot{V}_E , V_T , and V_T/T_I responses during severe hypercapnic hypoxia among F2 offspring to mouse chromosome 1. With peak LOD scores of 4.4, 4.2, and 4.9, respectively, these data strongly suggest that a putative QTL within the interval between 68 and 89 cM (i.e., between *D1Mit14* and *D1Mit291*) regulates C3 and B6 strain variation in ventilatory responses to high CO₂ levels in hypoxia.

Figure 6 illustrates LOD plots, suggesting that the variation on CO₂ potentiation phenotypes among F2 offspring are linked to mouse chromosome 5. With the use of the CO₂ gains from both \dot{V}_E and V_T/T_I responses, peak LOD scores of 3.7 and 3.5, respectively, suggest that at least one major genetic determinant modulates increased HCVS with hypoxia compared with normoxia. This genetic determinant is positioned on chromosome 5 in a region between 7 and 29 cM (i.e., centered at *D5Mit66*).

DISCUSSION

The results of the present study demonstrate two QTL on mouse chromosomes 1 and 5 that modulate variation in breathing responses associated with the interaction between hypoxic and hypercapnic challenge. The QTL on chromosome 1 links

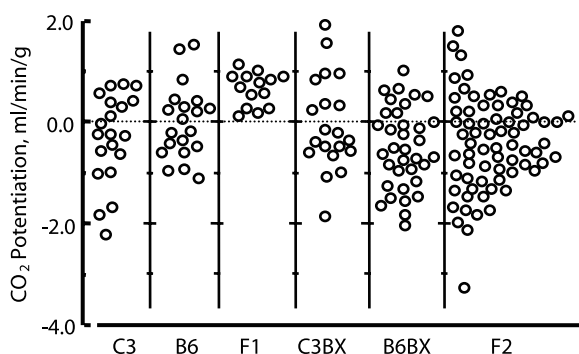


Fig. 4. A segregation plot of individual responses indicative of CO₂ potentiation is depicted for the C3 and B6 progenitors and their first- and second-generation offspring. The dotted-line demarcates the number of individual responses conferring CO₂ potentiation phenotypes. Because F1 responses consistently show CO₂ potentiation phenotypes, the data strongly suggest that heritable genetic determinants derived from C3 and B6 progenitors confer greater CO₂ ventilatory sensitivity during hypoxia relative to normoxia.

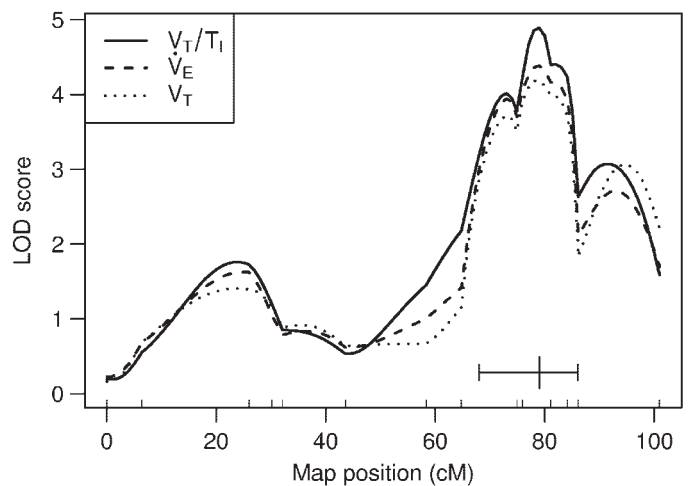


Fig. 5. LOD (i.e., log-likelihood) score graphs illustrate linkage results of F2 offspring ($n = 52$ mice) between DNA markers on mouse chromosome 1 and hypercapnic hypoxic \dot{V}_E , tidal volume (V_T), and V_T/T_I responses. The peak LOD score for each response is located within an interval between 68 and 89 cM from the centromere or between markers *D1Mit14* and *D1Mit291*. On the abscissa, the map position is indicated by both distance from the centromere along chromosome 1 (outside grid marks) and the DNA marker locations (inside grid marks).

variation in the \dot{V}_E , V_T , and V_T/T_I responses to a region between 68 and 89 cM or between markers *D1Mit14* and *D1Mit291*. The second QTL on mouse chromosome 5 links variation in CO₂ potentiation phenotypes to a region between 7 and 29 cM or centered at *D5Mit66*. The QTL on chromosomes 1 and 5 likely modulate separate aspects of the chemosensory or signal transduction mechanisms essential to the central integration of hypoxic and hypercapnic breathing. One substantial piece of evidence supporting this postulation suggest that C3 and B6 progenitor strains differ in their activation of the nucleus tractus solitarius (NTS) during hypercapnic challenge. The C3 strain exhibits a significantly lower activa-

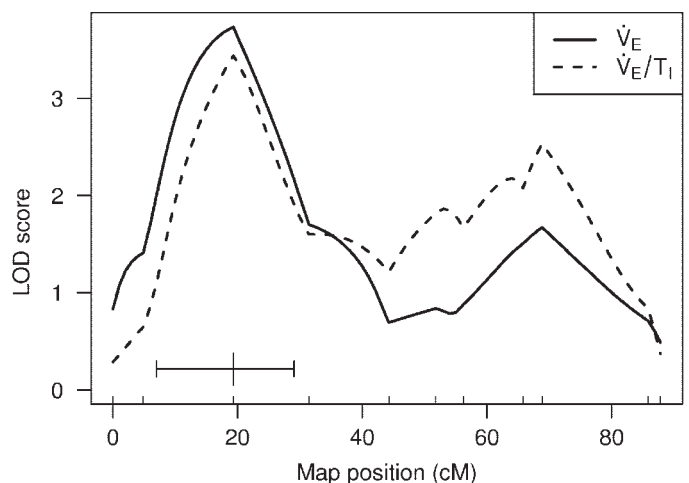


Fig. 6. LOD (i.e., log-likelihood) score graphs illustrate linkage results of F2 offspring ($n = 52$ mice) between DNA markers on mouse chromosome 5 and phenotypes indicative of CO₂ potentiation; i.e., using measurements of \dot{V}_E and V_T/T_I . The peak LOD score for each response is located within an interval between 7 and 29 cM or centered at marker *D5Mit66*. On the abscissa, the map position is indicated by both distance from the centromere along chromosome 5 (outside grid marks) and the DNA marker locations (inside grid marks).

tion on NTS neurons during hypercapnic stimulation compared with the B6 strain (41). The strain difference in CO₂-induced NTS activation is positively associated with the HCVS phenotypes (i.e., high gain in B6 and low gain in C3). Future studies are needed to identify the precise linkage between specific genes and the strain difference in chemosensory or signal transduction mechanisms between C3 and B6 mice.

Hypercapnic hypoxic breathing phenotype and chromosome 1. Hypercapnic hypoxic \dot{V}_E responses covaried with body weight within each parental strain (Fig. 2). After adjustment for variation in body weight, hypercapnic hypoxic \dot{V}_E and V_T/T_I responses remain ~40% greater in B6 compared with C3 mice. The hypercapnic hypoxic \dot{V}_E responses of F1 mice are unique relative to corresponding responses in the progenitors. At low CO₂ levels, the \dot{V}_E responses of F1 mice are parallel or attenuated relative to the C3 progenitor. For example, F1 mice demonstrated lower V_T and V_T/T_I responses to hypoxia relative to C3 mice at low CO₂ levels (34, 37). In contrast, \dot{V}_E and V_T/T_I responses of F1 mice are significantly amplified by hypoxia at high CO₂ levels, leading to an intermediate \dot{V}_E and V_T/T_I phenotype compared with the parental strains (Fig. 1). Therefore, the data fundamental to constructing HCVS curves in normoxia and hypoxia indicate another unique breathing phenotype in F1 mice by showing a consistently greater slope for HCVS with hypoxia. The CO₂ potentiation phenotype observed in F1 mice is not consistently seen in other inbred strains (35).

Approximately 150 known genes and other QTL are mapped in a proximal linkage region on mouse chromosome 1 between markers *DIMit14* and *DIMit291*, but only two genes are known to be polymorphic between these two progenitor strains (22a, 32). One construct, *Pou5F1-rs1*, is a related transcription factor to the *Pou5f1* gene, which is essential to early neural development (27). Its deletion adversely impacts peripheral nervous development, and breathing defects in mutant homozygotes are associated with a dramatically increased mortality risk (3). Another gene at the same map position (i.e., 84.6 cM) is the *Serpinc1* gene (28), which encodes for antithrombin III. There are a variety of human polymorphisms involving antithrombin III that are well studied related to thrombosis (2, 24). In mice, targeted gene disruption of the *Serpinc1* gene causes embryonic mortality due to dysfunctional blood coagulation in the heart (16). Other biologically plausible genes reside within the linkage region of mouse chromosome 1. A multigene family consisting of at least six different regulators of G-protein signaling is positioned at 78 cM in the mouse genome (31). For example, *Rgs2* gene expression is known to be rapidly responsive to dopamine D1 and D2 agonists (45) and to play a role in sensory experience-induced neural development (14) and neuronal plasticity (15). Two other genes in the region, *Cacnals* and *Cacna1e*, encode subunits of the R- and L-type voltage-dependent Ca²⁺ channels (18).

Alternative explanations to account for covariation between hypercapnic hypoxic \dot{V}_E responses and body weight include other QTL mapped to chromosome 1 associated with obesity. Three such QTL (i.e., *Bw17*, *Wt3q1*, and *Obq9*) confer obese phenotypes (1, 22, 44), whereas other genes (e.g., *Lmx1a* and *Hipp1*) confer variation in brain size or morphology (7, 19). Last, one gene (i.e., *Nidd6*) is associated with noninsulin-dependent diabetes, and another gene (i.e., *Amp2*) is linked to variation in circadian pattern (12, 30). In summary, the close

proximity of modulatory genes that affect obesity phenotypes, including diabetes and state-dependent behavior, may indicate a fundamental genetic basis for these phenotypes to covary with differences in ventilatory responses to chemical stimulation. Furthermore, the linkage region of interest on mouse chromosome 1 is highly conserved and mapped to human chromosome 1 (22a), suggesting that complex disease traits may originate from narrow genomic segments, and, as a result, act as comorbidity factors.

CO₂-potentiation phenotypes and chromosome 5. Masuda et al. (20) recently demonstrated potentiated CO₂ gain in humans, which ranged between end-tidal Pco₂ of 45 to >60 Torr. The CO₂ potentiation was observed at extreme inspirates of hypercapnia (F_ICO₂ = 0.07) with hyperoxic or hypoxic admixtures (F_IO₂ = 0.93 or 0.11, respectively). This control of breathing characteristic has been observed in other larger mammalian species (8) and implicates a synergy between CO₂ and O₂ chemosensory and transduction mechanisms, possibly arising from multiple peripheral and central chemoreceptor input. In a survey of the 10 standard inbred strains, only B6 mice were characterized as manifesting CO₂ potentiation. In the other strains, the interaction between hypoxic and hypercapnic ventilation appears to be more additive than synergistic (35). Given alternative definitions and phenotyping measurements (e.g., Ref. 46) to study the interactions between hypercapnic and hypoxia, CO₂ potentiation in mouse strains akin to breathing phenotypes in humans may become more evident.

Approximately 75 known genes and other QTL are currently identified in the linkage region of interest on mouse chromosome 5 (22a), and 4 genes are known to be polymorphic between C3 and B6 strains. Two polymorphic genes, *Htr5a* and *Adra2c*, have strong potential biological relevance to control of breathing, particularly related to the interaction between hypercapnic and hypoxic ventilation. The *Htr5a* gene encodes the 5-hydroxytryptamine (5-HT or serotonin) receptor 5A, and the *Adra2c* gene encodes a subunit of the α_2 -adrenergic receptor. Both genes are located within 2–3 cM of the peak LOD score for the QTL-modulating variation in CO₂ potentiation. The *Htr5a* gene is a relatively new clone, and its relevance to the control of breathing is not well established. However, in goats, the acute hypoxic ventilatory response is augmented by broad-spectrum serotonergic blockade, but the 5-HT(1A) and 5-HT(2A/C) receptors do not appear to mediate the augmented response (11), leaving open the possibility that alternative 5-HT receptor subtypes are influential in acute hypoxic \dot{V}_E responses. Serra et al. (29) showed that the ventilatory response to aortic chemoreceptor stimulation is mediated by 5-HT(5A) receptors in rats and piglets. The immunoreactive site for an abundance of 5-HT(5A) receptors was concentrated on the aortic chemosensitive sites (29). Therefore, the questionable role of 5-HT(5A) receptors in regulating variation in CO₂ potentiation requires greater study.

The function of α_2 -adrenergic receptor stimulation in the control of breathing leads to an inhibition of f . This tonic inhibition of f is partially mediated by the α_2 -adrenergic receptor subtype 2C in goats (23). The novel phenotype of CO₂ potentiation manifested by F1 mice in the present study results from a breathing strategy in which both f and V_T components increase from normoxia to hypoxia. The f -dependent increase is likely derived from the C3 parental strain, whereas the

V_T-dependent increase is derived from the B6 parental strain. The C3 and F1 mice may generate a relatively greater tachypnea, with hypoxia involving differential interactions between α_2 -adrenergic receptor subtypes. O'Halloran et al. (23) demonstrated a greater isocapnic hypoxic \dot{V}_E response after blockade of these specific α_2 -adrenergic receptor subtypes. This investigative team suggested that the likely roles of α_2 -adrenergic receptors in potentiating the hypoxic \dot{V}_E responses occur either by increasing carotid body chemosensitivity or by altered chemoafferent fibers that synapse at the NTS, which affects central integration of several chemosensitive inputs. Although Bissonnette et al. (4) demonstrated ventilatory aberrations in mice lacking functional α_{2A} -adrenergic receptors, the role of subtype 2C receptors remains undefined. One study by Puolivali et al. (25) suggested that α_{2C} -adrenergic receptors mediated arousal and counterbalance the sedation effects of α_{2A} -adrenergic receptor activation. This potential mechanism may involve the central integration of breathing as it relates to sleep and arousal state.

In summary, present results demonstrate that QTL on mouse chromosomes 1 and 5 interact to affect breathing responses during acute hypercapnic and hypoxic challenges. There is definitive strain variation between C3 and B6 mice in the magnitude and pattern of breathing during hypercapnic hypoxia, and the F1 inherit different parental phenotypes that embody the characteristic of CO₂ potentiation. Candidate genes in the linkage region on mouse chromosome 1, regulating variation in \dot{V}_E , V_T, and V_T/T_I responses during hypercapnic hypoxia, remain relatively obscure. Alternatively, two genes on mouse chromosome 5, *Htr5a* and *Adra2c*, encode relevant neuroreceptor subtypes involved in serotonergic and adrenergic pathways, which potentially regulate breathing. These two candidate genes are also known to be polymorphic between C3 and B6 mice. Although it is clear that the physiological mechanisms synchronizing the regulation of breathing during hypercapnic hypoxia are complex, the corresponding genetic interactions may represent one source of variation in unique breathing outcomes.

ACKNOWLEDGMENTS

The authors gratefully acknowledge the technical assistance of Heather Kulaga and Alexis Bierman, and the cooperation of the Department of Anesthesiology at the Johns Hopkins School of Medicine.

GRANTS

This study was supported by National Heart, Lung, and Blood Institute Grant HL-53700.

REFERENCES

- Anunciado RV, Nishimura M, Mori M, Ishikawa A, Tanaka S, Horio F, Ohno T, and Namikawa T. Quantitative trait loci for body weight in the intercross between SM/J and A/J mice. *Exp Anim* 50: 319–324, 2001.
- Beresford CH. Antithrombin III deficiency. *Blood Rev* 2: 239–250, 1988.
- Birmingham JRJ, Scherer SS, O'Connell S, Arroyo E, Kalla KA, Powell FL, and Rosenfeld MG. Tst-1/Oct-6/SCIP regulates a unique step in peripheral myelination and is required for normal respiration. *Genes Dev* 10: 1751–1762, 1996.
- Bissonnette JM, Knopp SJ, Wright DM, and MacMillan LB. Respiratory pattern and hypoxic ventilatory response in mice functionally lacking α_{2A} -adrenergic receptors. *Adv Exp Med Biol* 499: 201–208, 2003.
- Broman KW, Wu H, Sen S, and Churchill GA. R/qtl: QTL mapping in experimental crosses. *Bioinformatics* 19: 889–890, 2003.
- Bulchand S, Subramanian L, and Tole S. Dynamic spatiotemporal expression of LIM genes and cofactors in the embryonic and postnatal cerebral cortex. *Dev Dyn* 226: 460–469, 2003.
- Carroll JL, Bamford OS, and Fitzgerald RS. Postnatal maturation of carotid chemoreceptor responses to O₂ and CO₂ in the cat. *J Appl Physiol* 75: 2383–2391, 1993.
- Churchill GA and Doerge RW. Empirical threshold values for quantitative trait mapping. *Genetics* 138: 963–971, 1994.
- Fitzgerald RS and Parks DC. Effect of hypoxia on carotid chemoreceptor response to carbon dioxide in cats. *Respir Physiol* 12: 218–229, 1971.
- Herman JK, O'Halloran KD, and Bisgard GE. Effect of 8-OH DPAT and ketanserin on the ventilatory acclimatization to hypoxia in awake goats. *Respir Physiol* 124: 95–104, 2001.
- Hirayama I, Yi Z, Izumi S, Arai I, Suzuki W, Nagamachi Y, Kuwano H, Takeuchi T, and Izumi T. Genetic analysis of obese diabetes in the TSOD mouse. *Diabetes* 48: 1183–1191, 1999.
- Ihaddad R and Gentleman R. R: a language for data analysis and graphics. *J Computat Graphical Stat* 5: 299–314, 1996.
- Ingi T and Aoki Y. Expression of RGS2, RGS4 and RGS7 in the developing postnatal brain. *Eur J Neurosci* 15: 929–936, 2002.
- Ingi T, Krumins AM, Chidiac P, Brothers GM, Chung S, Snow BE, Barnes CA, Lanahan AA, Siderovski DP, Ross EM, Gilman AG, and Worley PF. Dynamic regulation of RGS2 suggests a novel mechanism in G-protein signaling and neuronal plasticity. *J Neurosci* 18: 7178–7188, 1998.
- Ishiguro K, Kojima T, Kadomatsu K, Nakayama Y, Takagi A, Suzuki M, Takeda N, Ito M, Yamamoto K, Matsushita T, Kusugami K, Muramatsu T, and Saito H. Complete antithrombin deficiency in mice results in embryonic lethality. *J Clin Invest* 106: 873–878, 2000.
- Kobayashi S, Nishimura M, Yamamoto M, Akiyama Y, Kishi F, and Kawakami Y. Dyspnea sensation and chemical control of breathing in adult twins. *Am Rev Respir Dis* 147: 1192–1198, 1993.
- Lee SC, Choi S, Lee T, Kim HL, Chin H, and Shin HS. Molecular basis of R-type calcium channels in central amygdala neurons of the mouse. *Proc Natl Acad Sci USA* 99: 3276–3281, 2002.
- Lu L, Airey DC, and Williams RW. Complex trait analysis of the hippocampus: mapping and biometric analysis of two novel gene loci with specific effects on hippocampal structure in mice. *J Neurosci* 21: 3503–3514, 2001.
- Masuda A, Ohyabu Y, Kobayashi T, Yoshino C, Sakakibara Y, Komatsu T, and Honda Y. Lack of positive interaction between CO₂ and hypoxic stimulation for PCO₂-VAS response slope in humans. *Respir Physiol* 126: 173–181, 2001.
- Milic-Emili J and Grunstein MM. Drive and timing components of ventilation. *Chest* 70: 131–133, 1976.
- Moody DE, Pomp D, Nielsen MK, and Van Vleck LD. Identification of quantitative trait loci influencing traits related to energy balance in selection and inbred lines of mice. *Genetics* 152: 699–711, 1999.
- 22a. Mouse Genomic Database (MGD), Mouse Genome Informatics. Bar Harbor, ME: Jackson Lab., 2003.
- O'Halloran KD, Herman JK, and Bisgard GE. Ventilatory effects of α_2 -adrenergic receptor blockade in awake goats. *Respir Physiol* 126: 29–41, 2001.
- Perry DJ and Carrell RW. Molecular genetics of human antithrombin deficiency. *Hum Mutat* 7: 7–22, 1996.
- Puolivali J, Bjorklund M, Holmberg M, Ihalainen JA, Scheinin M, and Tanila H. α_{2C} -Adrenoceptor mediated regulation of cortical EEG arousal. *Neuropharmacology* 43: 1305–1312, 2002.
- Sambrook J, Fritsch EF, and Maniatis T. *Molecular Cloning: A Laboratory Manual*. New York: Cold Spring Harbor, 1989.
- Schonemann MD, Ryan AK, Erkman L, McEvilly RJ, Birmingham J, and Rosenfeld MG. POU domain factors in neural development. *Adv Exp Med Biol* 449: 39–53, 1998.
- Seldin MF, Morse HC, Reeves JP, Scribner CL, LeBoeuf RC, and Steinberg AD. Genetic analysis of autoimmune gld mice. I. Identification of a restriction fragment length polymorphism closely linked to the gld mutation within a conserved linkage group. *J Exp Med* 167: 688–693, 1988.
- Serra A, Brozoski D, Simeon T, Yi J, Bastasic J, Franciosi R, Jacobs ER, and Forster HV. Serotonin and serotonin receptor expression in the aorta of carotid intact and denervated newborns. *Respir Physiol Neurobiol* 132: 253–264, 2002.
- Shimomura K, Low-Zeddies SS, King DP, Steeves TD, Whiteley A, Kushla J, Zemenides PD, Lin A, Vitaterna MH, Churchill GA, and Takahashi JS. Genome-wide epistatic interaction analysis reveals complex genetic determinants of circadian behavior in mice. *Genome Res* 11: 959–980, 2001.

31. **Sierra DA, Gilbert DJ, Householder D, Grishin NV, Yu K, Ukidwe P, Barker SA, He W, Wensel TG, Otero G, Brown G, Copeland NG, Jenkins NA, and Wilkie TM.** Evolution of the regulators of G-protein signaling multigene family in mouse and human. *Genomics* 79: 177–185, 2002.
32. **Siracusa LD, Rosner MH, Viganò MA, Gilbert DJ, Staudt LM, Copeland NG, and Jenkins NA.** Chromosomal location of the octamer transcription factors, Otf-1, Otf-2, and Otf-3, defines multiple Otf-3-related sequences dispersed in the mouse genome. *Genomics* 10: 313–326, 1991.
33. **Tankersley CG.** A genomic model for differential hypoxic ventilatory responses. *Adv Exp Med Biol* 475: 75–85, 2000.
34. **Tankersley CG.** Selected Contribution: Variation in acute hypoxic ventilatory response is linked to mouse chromosome 9. *J Appl Physiol* 90: 1615–1622, 2001.
35. **Tankersley CG.** Genetic aspects of breathing: on interactions between hypercapnia and hypoxia. *Respir Physiol Neurobiol* 135: 167–178, 2003.
36. **Tankersley CG, DiSilvestre DA, Jedlicka AE, Wilkins HM, and Zhang L.** Differential inspiratory timing is genetically linked to mouse chromosome 3. *J Appl Physiol* 85: 360–365, 1998.
37. **Tankersley CG, Elston RC, and Schnell AH.** Genetic determinants of acute hypoxic ventilation: patterns of inheritance in mice. *J Appl Physiol* 88: 2310–2318, 2000.
38. **Tankersley CG, Fitzgerald RS, and Kleeberger SR.** Differential control of ventilation among inbred strains of mice. *Am J Physiol Regul Integr Comp Physiol* 267: R1371–R1377, 1994.
39. **Tankersley CG, Fitzgerald RS, Levitt RC, Mitzner WA, Ewart SL, and Kleeberger SR.** Genetic control of differential baseline breathing pattern. *J Appl Physiol* 82: 874–881, 1997.
40. **Tankersley CG, Kulaga H, and Wang MM.** Inspiratory timing differences and regulation of Gria2 gene variation: a candidate gene hypothesis. *Adv Exp Med Biol* 499: 477–482, 2001.
41. **Tankersley CG, Haxhiu MA, and Gauda EB.** Differential CO₂-induced c-fos gene expression in the nucleus tractus solitarius of inbred mouse strains. *J Appl Physiol* 92: 1277–1284, 2002.
42. **Tankersley CG, Irizarry R, Flanders S, and Rabold R.** Circadian rhythm variation in activity, body temperature, and heart rate between C3H/HeJ and C57BL/6J inbred strains. *J Appl Physiol* 92: 870–877, 2002.
43. **Tankersley CG, Rabold R, and Mitzner W.** Differential lung mechanics are genetically determined in inbred murine strains. *J Appl Physiol* 86: 1764–1769, 1999.
44. **Taylor BA, Wnek C, Schroeder D, and Phillips SJ.** Multiple obesity QTLs identified in an intercross between the NZO (New Zealand obese) and the SM (small) mouse strains. *Mamm Genome* 12: 95–103, 2001.
45. **Taymans JM, Leysen JE, and Langlois X.** Striatal gene expression of RGS2 and RGS4 is specifically mediated by dopamine D1 and D2 receptors: clues for RGS2 and RGS4 functions. *J Neurochem* 84: 1118–1127, 2003.
46. **Yamaguchi S, Balbir A, Schofield B, Coram J, Tankersley CG, Fitzgerald RS, O'donnell CP, and Shirahata M.** Structural and functional differences of the carotid body between DBA/2J and A/J strains of mice. *J Appl Physiol* 94: 1536–1542, 2003.
47. **Zeng ZB.** Theoretical basis for separation of multiple linked gene effects in mapping quantitative trait loci. *Proc Natl Acad Sci USA* 90: 10972–10976, 1993.
48. **Zeng ZB.** Precision mapping of quantitative trait loci. *Genetics* 136: 1457–1468, 1994.

